# SIMULATIONS OF SHOCK GENERATION AND PROPAGATION IN POROUS MEDIA FOR LASER-PLASMA EXPERIMETS.

N.G. Borisenko[1)], A.I. Lebo[2)], I.G. Lebo[3)], Yu.A. Merkul'ev[1)]

[1)] *Lebedev Physical Institute, Leninski prospect, 53, Moscow, Russia*

[2)] *Lomonosov Moscow State University, Vorobyevi gori 1, 119234 Moscow, Russia*

[3)] *Technical University–MIREA, Prospect Vernadskogo 78, 119454 Moscow, Russia*

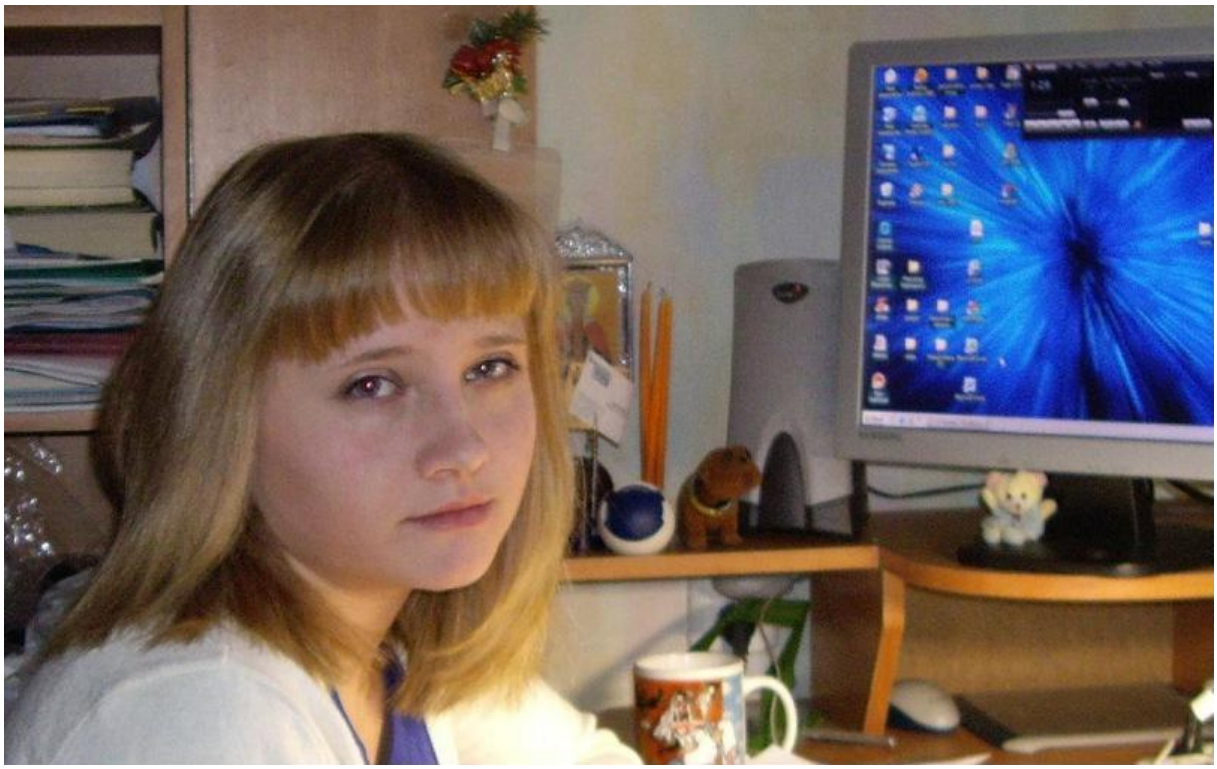

## Abstract

We have considered the physical-mathematical model of compression wave formation and propagation in low density matter initiated by power laser pulse. Initial density of such matter has been less then critical density for laser irradiation with wavelength 0,438 μm. The laser target has consisted of two layers: Al base with thickness of 5 μm and porous polymer matter with thickness of a few hundred microns. Using 2D "ATLANT" code we have made the numerical calculations of physical processes in such matter. The results these calculations have been compared with the

experimental data from PALS laboratory experiments (Prague, CZ). The thickness of porous target is similar of laser spot scale. In these conditions we have studied the effect of 2D geometry on the expansion of shock wave in low density targets. W have got the following dependence of average compression wave velocity from initial density: $\overline{V} \sim \rho_0^{\alpha}$ , where $\rho_0$ – initial density of porous media, $\alpha \approx (0.25\text{-}0.45)$. The part of laser energy has come through the low-density matter at the initial stage and heated Al base. As the results of two plasma flow collision the hydro-thermal wave comes to the rear side of aluminium layer much later of laser pulse finish.

## The short description of experimental data.

Energy transport velocities in under critical plasmas from polymer aerogel were measured at the $I_2$-laser "PALS" (Prague, CZ [1]). Laser light of wavelength 0,438 μm, intensity $(3\text{-}7)\cdot 10^{14}$ W/cm$^2$ and ~0,8 ns pulse duration was used to study of wave expansion in porous media. Fig.1 shows the scheme of diagnostic complex at "PALS" installation.

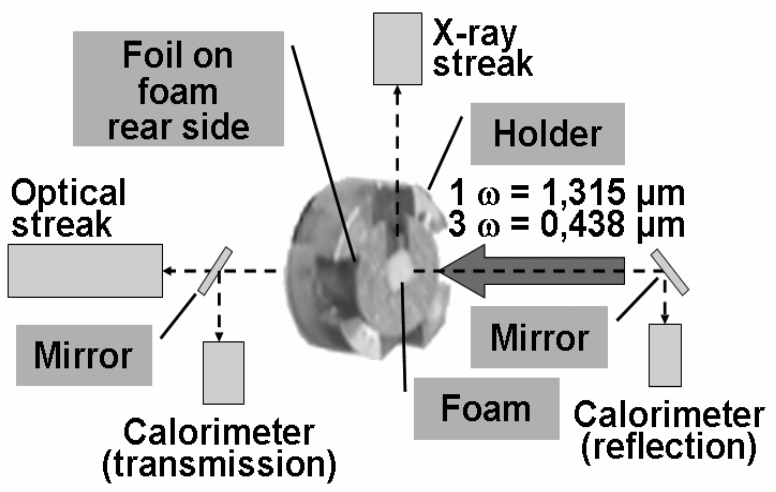


*FIG.1. The scheme of diagnostic complex.*

The first calorimeter has measured the reflected laser energy, the second calorimeter has measured the transmission laser beam energy through the porous matter.

It has been measured the transmission of laser light transmission through the porous layer with thickness 100, 200 and 400 μm for initial average densities $\rho_0$=9 mg/cm$^3$ $\rho_0$=4.5 mg and $\rho_0$=2.25 mg/cm$^3$. The porous matter puts on the aluminum base with thickness about 5 μm.

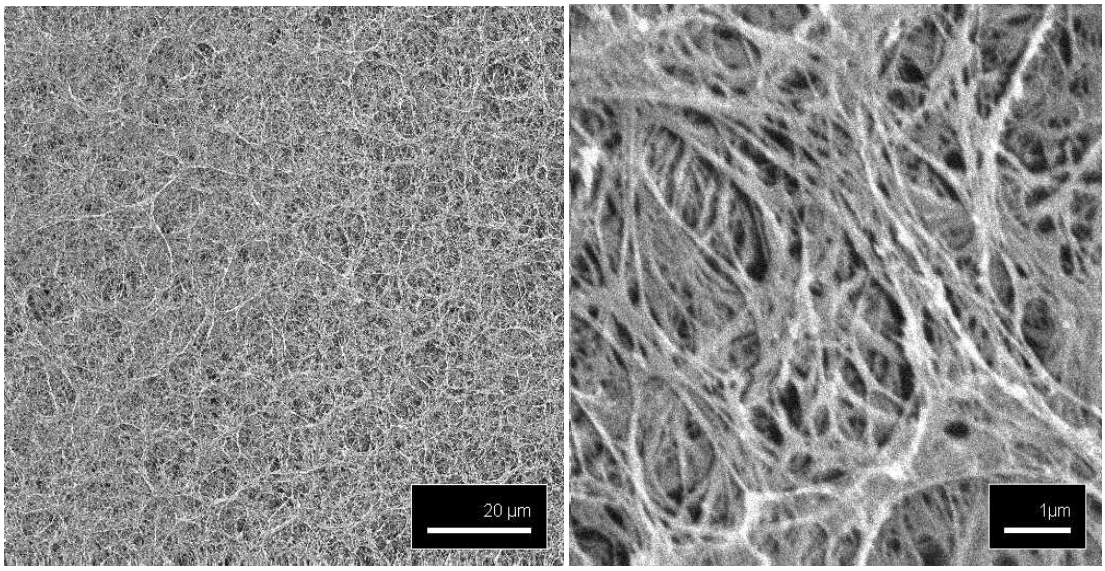


*FIG.2. Structure of porous matter. The picture has made by use electron microscope.*

**Table 1**. The transmission of laser energy ( % to fall laser energy), through the porous matter with different initial density for laser intensity: (6-8)·$10^{14}$ W/cm$^2$ и (3-4)·$10^{14}$ W/cm$^2$

| ↓ Density \ thickness → | 400 µm | 200 µm | 100 µm |
|---|---|---|---|
| *9 mg/cm$^3$ | 3,0% | 6.2% | 13% |
| *4.5 mg/cm$^3$ | 8.7% | 21% | 47% |
| *2.25 mg/cm$^3$ | 29% | 42% | - |
| **4.5 mg/cm$^3$ | 8% | 16% | 37% |
| **2.25 mg/cm$^3$ | 13% | 25% | 53% |

*Laser intensity (6-8)·$10^{14}$ W/cm$^2$
**Laser intensity (3-4)·$10^{14}$ W/cm$^2$

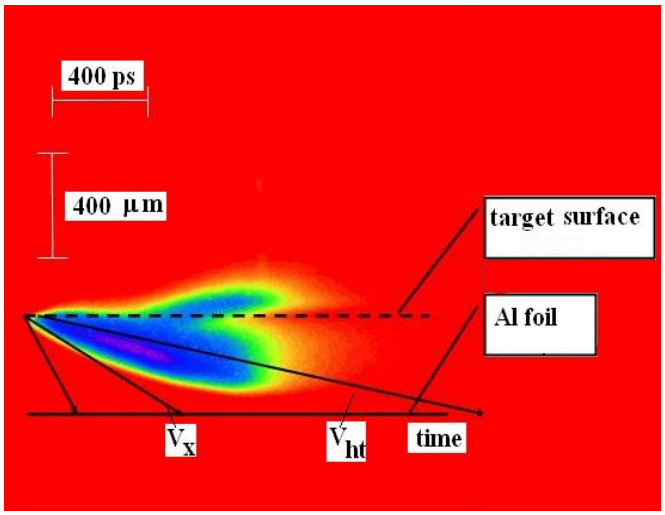


*Fig.3. The image of porous target emission, $V_x$ – X ray front formation velocity, $V_{ht}$ – maximal brightness velocity*

The time dependences of optical emission from the rear side of two-layer target (aerogel layer with thickness 400 μm and different densities plus Al-foil with thickness 5 μm) give the data of wave velocities(in detail see [2]). Such emission was observed usually when laser pulse had been finished.

The numerical simulation of wave expansion were made by using “ATLANT”-code.

## The basic physical-mathematical model.

2D Lagrangian code “ATLANT” in cylindrical geometry (cords: r, z and t). In details, see *I.G. Lebo & V.F. Tishkin “Issledovanie gidrodinamicheskoj neustojchivosti v zadachah lazernogo termojadernogo sinteza”, Monograph, Moscow, FIZMATLIT, 2006 ( in Russian).*

$$\frac{d\rho}{dt} = -\rho\vec{\nabla}\vec{v}$$

$$\rho\frac{d\vec{v}}{dt} = -\vec{\nabla}(Z_i \cdot P_E + P_I + P_R)$$

$$Z_i\rho\frac{dE_E}{dt} = -Z_i \cdot P_E\vec{\nabla}\vec{v} + \vec{\nabla}(\kappa_E\vec{\nabla}T_E) - Q_{EI} - Q_{ER} - R_{RAD}(\rho, T_E) + \vec{\nabla}\vec{q}$$

$$\rho\frac{dE_I}{dt} = -P_I\vec{\nabla}\vec{v} + \vec{\nabla}(\kappa_I\vec{\nabla}T_I) + Q_{EI}$$

$$\rho\frac{dE_R}{dt} = -P_R\vec{\nabla}\vec{v} + \vec{\nabla}(\kappa_R\vec{\nabla}T_R) + Q_{ER}$$

$$\left(\frac{\vec{q}}{|\vec{q}|}, \vec{\nabla}\right)\vec{q} = k(\rho, T_E)\cdot\vec{q}$$

$$Q_{EI} = Q_0(\rho, T_E)\frac{T_E - T_I}{T_E^{3/2}}\rho^2$$

$$P_E = P_E(\rho, T_E);\ P_I = P_I(\rho, T_I);\ P_R = P_R(\rho, T_R)$$

$$E_E = E_E(\rho, T_E);\ E_I = E_I(\rho, T_I);\ E_R = E_R(\rho, T_R)$$

Equation of state (EOS) is perfect plasma (without ionization and recombination processes, charges of ions are constant).

We do not take into account for radiative transport ($T_r$ =0).

## The results of numerical simulations.

The first set of simulations has modeled the expansion of shock wave in low density CH gas (initial density of the gas is $\rho_0$=9 mg/cm$^3$).

The target has two layers: outer low density layer and Al base (see Fig4a). The radius of calculation area is $R_0$ = 200 μm. The laser beam falls from right to left. The absorbed laser energy is $E_L$=170 J, pulse duration is τ=0,8 ns (see Fig4b) We have made "quasi-one dimensional" simulation, when laser intensity is not depend on radius, and numerical grid has only two Lagrange cell in transverse direction.

Variant 1: We have used the inverse bremsstrahlung mechanism of laser absorption in "ATLANT" model. Fig.4 illustrates the statement of problem and numerical results.

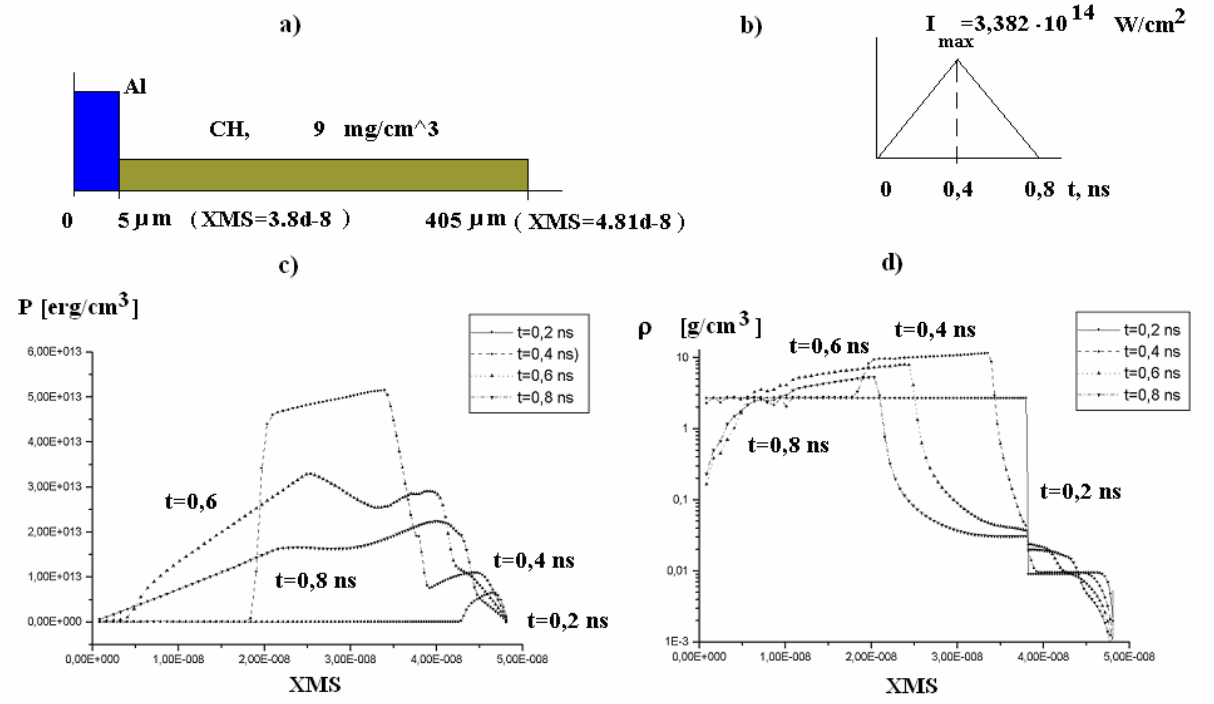


*Fig.4. The scheme of target (a) and laser pulse shape (b) and pressures (P) and densities (ρ) profiles as function of time.*

The mass cords: $XMS = \sum_{j=1}^{n} \Delta M_{2j}$ is postponed. Here $\Delta M_{ij}$ – the mass of Lagrange cells, (i=2-cells at an axis 0Z), n-number of a cell, where the portion of the absorbed power of laser radiation is defined.

The wave comes through the low density substance and Al foil with large velocity (it has reached the rear side of Al layer to the time moment t≈0,5 ns!)

Variant 3: we have compared the wave velocities with the case of solid target.

Two layers: Al+CH, but outer layer – solid CH ($\rho_0$=1 g/cm$^3$) with the mass, which is equal of the mass of porous media (see Fig.5a).

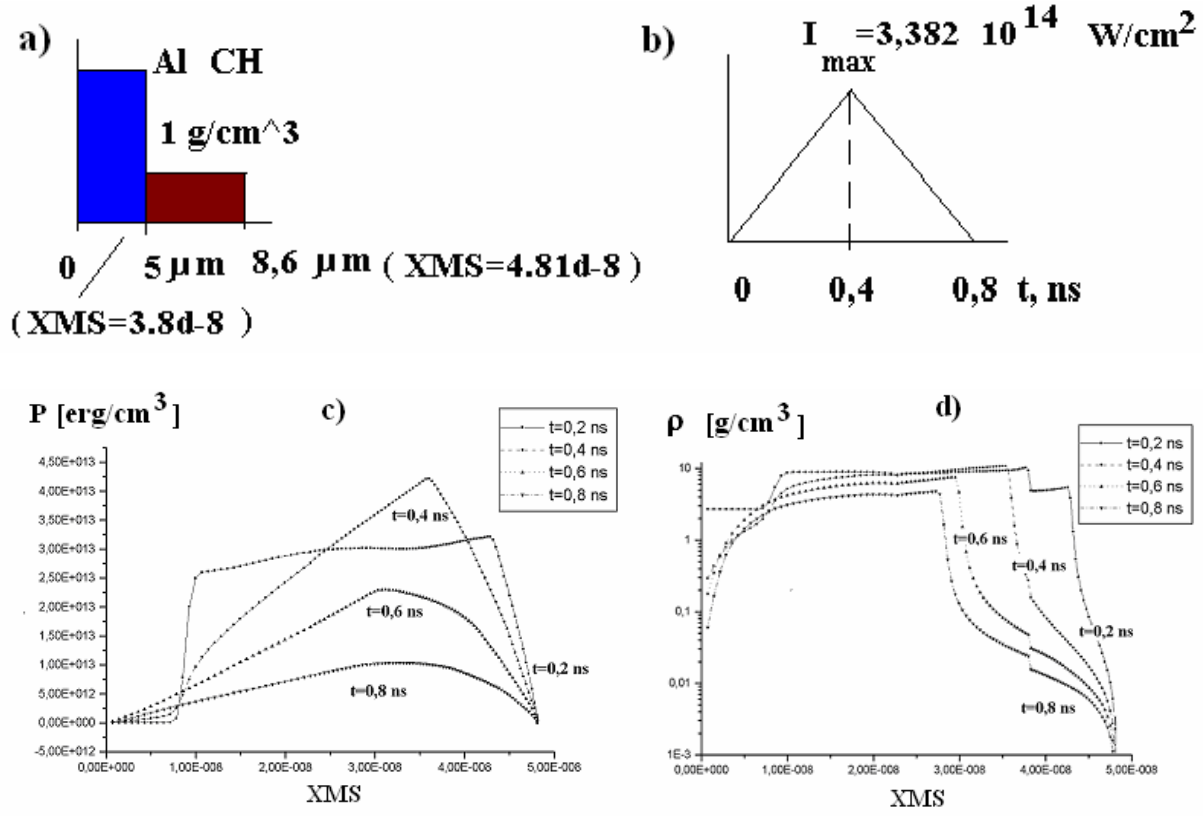


*Fig.5. The statement of problem: target scheme (a) and laser pulse shape (b). The numerical results: pressure (c) and density (d) distribution along 0Z axes.*

In this case the wave has reached the rear side of Al layer to the moment t≈0,4 ns too.

We have suppressed the thermal conductivity in $10^3$ times (!) and have made simulations with two layer target with low-density substance (see Fig.4a). The laser beam comes through the low density substance and initiates shock wave in Al layer This shock reaches the rear side of Al foil to the moment 0,55 ns. The basic reason of such effect: the coefficient of inverse bremstrallung absorption is $\chi_L \sim \frac{\rho^2}{T_e^{1.5}}$, and thermal

capacity is small. As the results, the temperature of low density substance has increased very fast and the hot plasma becomes transparent for laser beam.

Variants 17-19. We have tried to use another model of porous matter: there are a few solid thin layers in low density gas, and thermal conductivity is suppressed (variants 17-19). Fig.6 illustrates the results of the simulations.

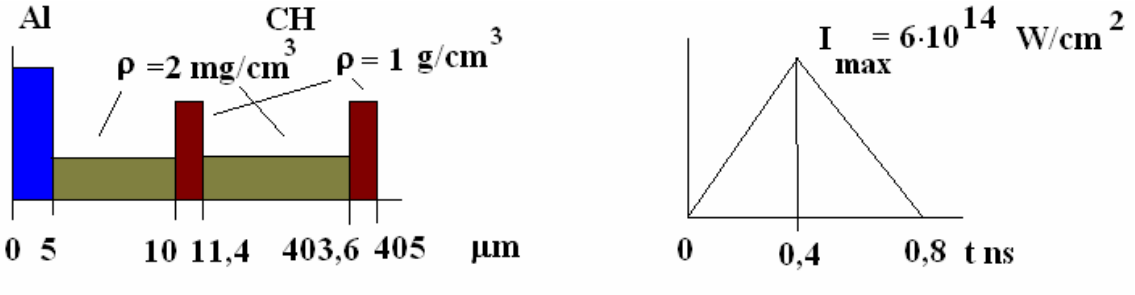


*Fig.6a,b. The scheme of target (a), the shape of laser pulse (b). The mass of target is equal of the mass of targets in variants 1-3.*

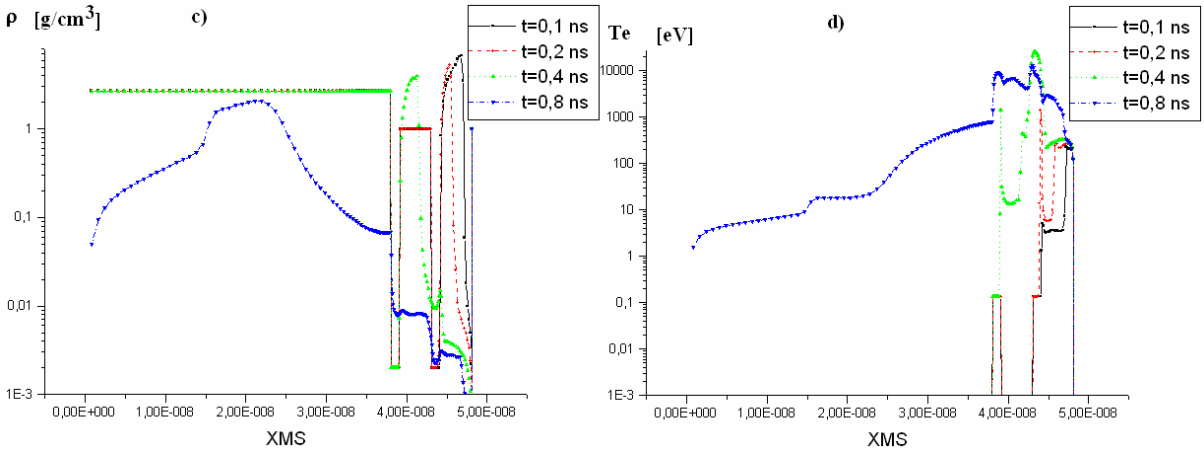


*Fig.6c,d. The density (c) and temperature (d) distributions along 0Z axes for different time moments.*

The shock wave reaches the rear side of Al layer to t= 0,7 ns. At the moment t=0,8 ns we have observed the rarefaction wave, which moves from rear side of Al layer.

We have carried out two-dimensional simulations of the target evolution in these variants. The laser flow is $q(t,r) = q_1(t) \cdot q_2(r)$, and $q_2(r) = 1./\exp(r/R_f)^2$, where $R_f$=150 μm, $R_0$=300 μm. The total laser energy is 170 J.

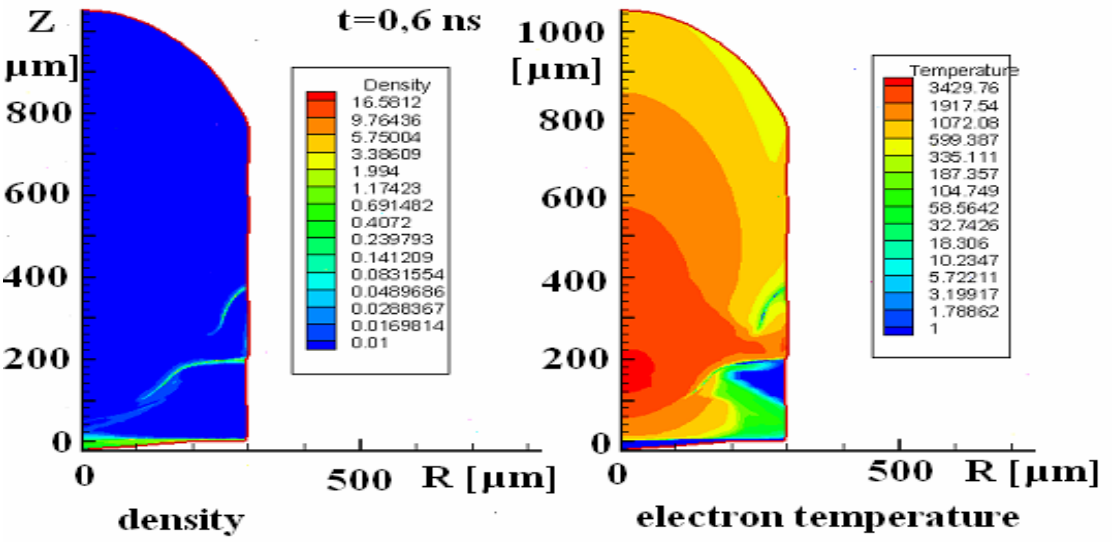


*Fig. 6e,f. Plasma density shape (left figure) and plasma temperature (right figure).*

In this case the laser flux comes through the porous media up to the moment t= 0,6 ns.

All variants show that: it needs to change the model of laser absorption in low density substance!

We have made the following changes in the model:

1. The coefficients of electron and ion thermal conductivities have been suppressed in low density substance is $(\chi_e = 10^{-3} \cdot \chi_{Sp\_e}, \chi_i = 10^{-2} \chi_{Sp\_i})$, where $\chi_{Sp\_e(i)}$ - "Spitzer values" of the coefficients.

2. The low of laser absorption is $\frac{\partial q_{Las}}{\partial z} = -\chi_L q_{Las}$, $\chi_L = \frac{\rho(z,t)}{\rho_0 l_a}$, where $\rho$, $\rho_0$- current and initial value of density, $l_a$ – some parameters We have taken $l_a = 1$ µm in our calculations.

Variants 15a-16a-23a. The next figure illustrates the expansion of compression wave in low-density substance for the variants 16a, 15a and 23a. The mass of low density layers are the same, but initial densities and the thicknesses are varied. At first, we have supposed, that the wave velocity depends only on the parameter:, where Z – thickness of low density substance.

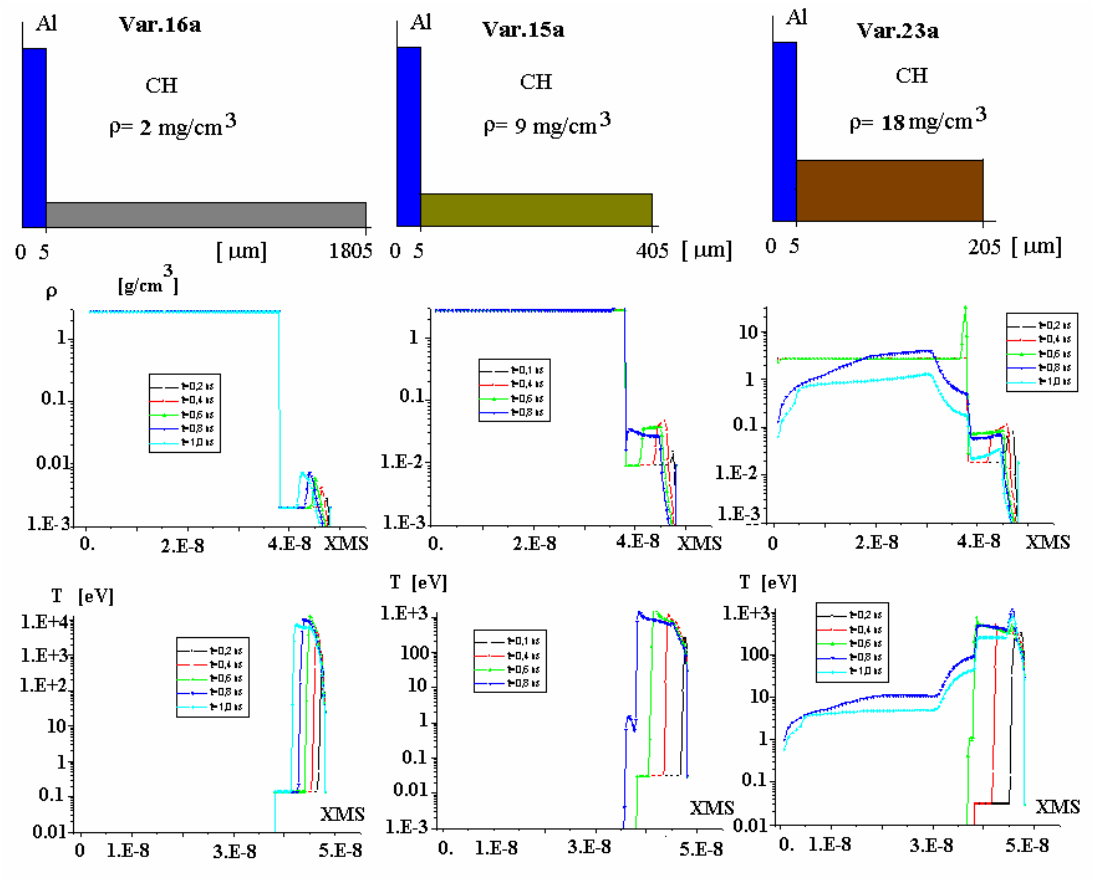


*Fig.7. Upper lever: schemes of targets for the variants 16a ($\rho_0$=2 mg/cm$^3$), 15a ($\rho_0$=9 mg/cm$^3$) and 23a ($\rho_0$=18 mg/cm$^3$), density distribution along the 0Z axes (the middle level) and temperature distributions along the 0Z axes (low level) for different time moments. XMS – is mass cords.*

As following from Fig.7 the dependence of wave velocity is more complicate.

Variants 25a, 15a, 24a. Next figure illustrates the wave expansion in variants 25a ($\rho_0$=4.5 mg/cm$^3$), 15a ($\rho_0$=9 mg/cm$^3$) and 24a ($\rho_0$=18 mg/cm$^3$). In these variants the thicknesses of low density substance are 400 μn. It suits the experimental data. It can see, that velocity propagation has diminished in compare with old model of laser absorption, but in the case of initial density $\rho_0 \le 4.5$ mg/cm$^3$ the "hydro-thermal wave" has reached aluminum layer before laser pulse finish (see Fig8, var.25a)

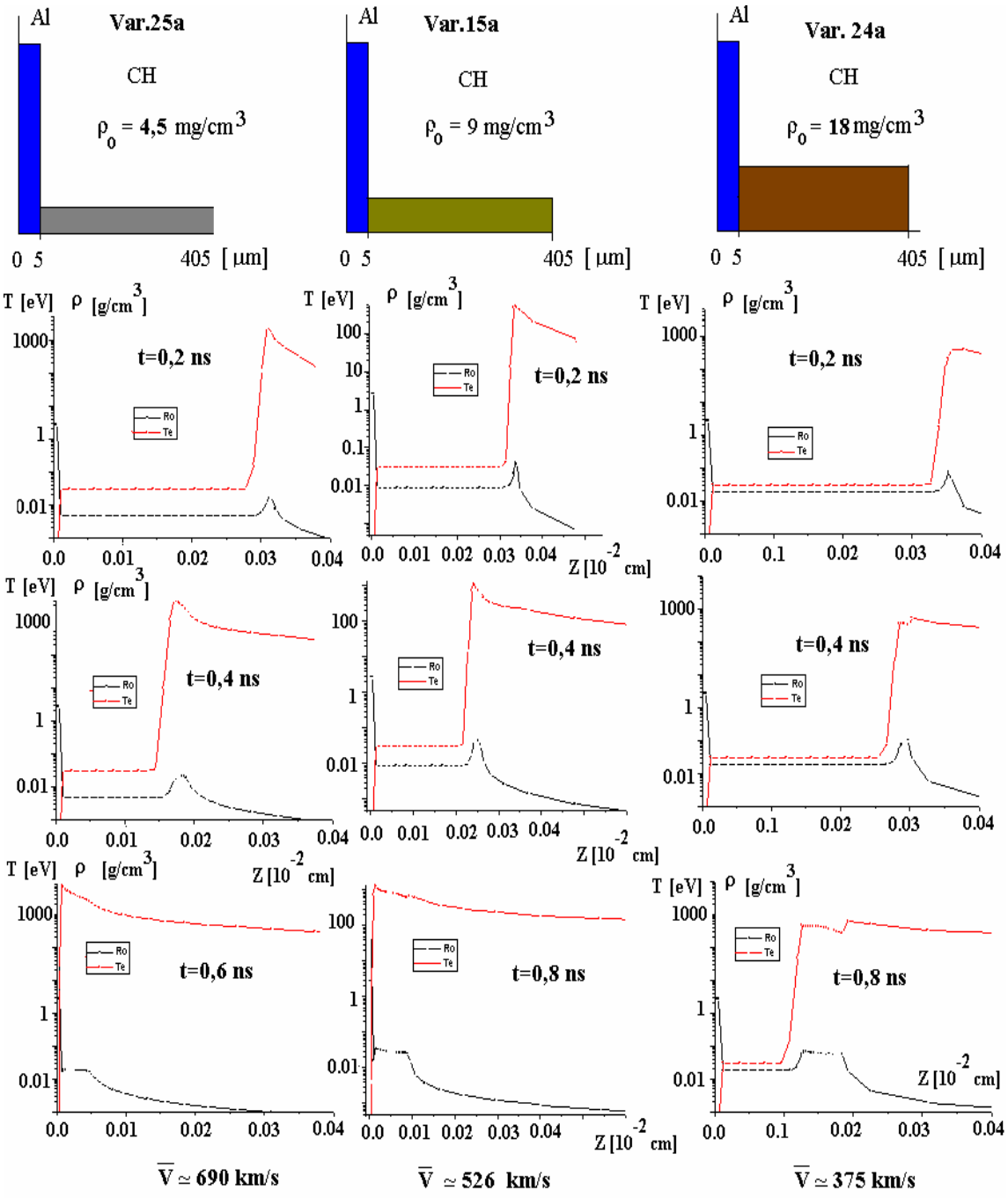


*Fig.8. Upper level: the schemes of targets. The suitable initial densities are 4.5 (variant 25a), 9 (variant 15a) and 18 mg/cm$^3$ (variant 24a). The distributions of temperature (red lines) and density (black line) along 0Z axis for the time moments t=0,2 ns, t=0,4 ns and when wave reaches Al foil (variants 25a and 15a).*

The average velocities of wave propagation in low density substances are $\overline{V} = 690$ km/s (variant 25a), $\overline{V} = 526$ km/s (variant 15a) and $\overline{V} = 375$ km/s (variant 24a).

The diameters of focal spots in the experiments are 300 μm and the thickness of porous matter is about 400 μm. In these conditions the influence of two-dimensional effects are important. We have made 2D simulations of variants 26a (initial density $\rho_0$=2.25 mg/cm$^3$), variant 25a ($\rho_0$=4.5 mg/cm$^3$), variant 15a ($\rho_0$=9 mg/cm$^3$) and variant 24a ($\rho_0$=18 mg/cm$^3$). Fig.9a illustrates the statement of 2D problem.

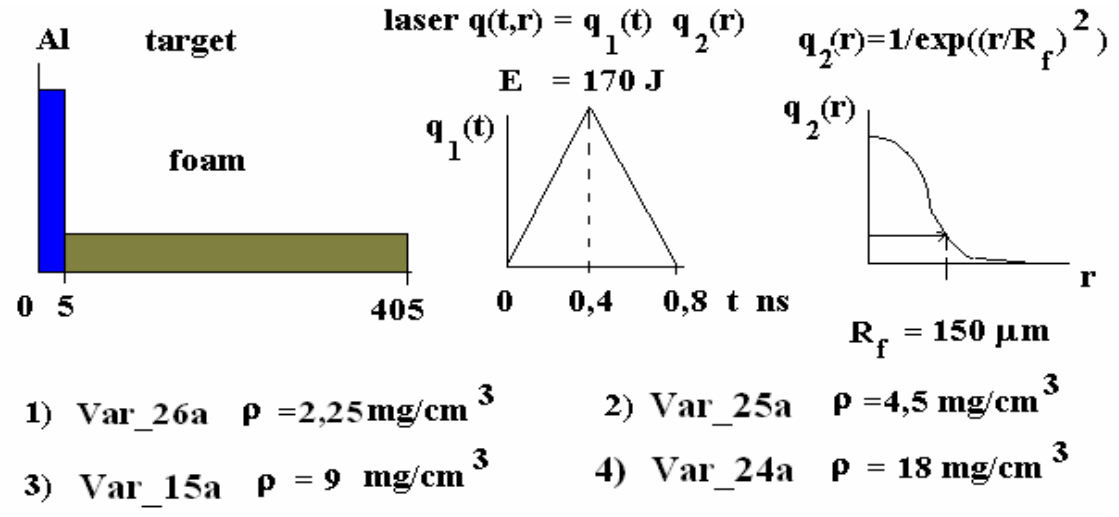


Fig.9a. Scheme of target (left figure) and the distributions of laser intensity (right figure).

The transverse radius of calculation area is $R_0$=600 μm. We have used nonregular numerical grid to increase the decision of calculations near the axis (see Fig.9b).

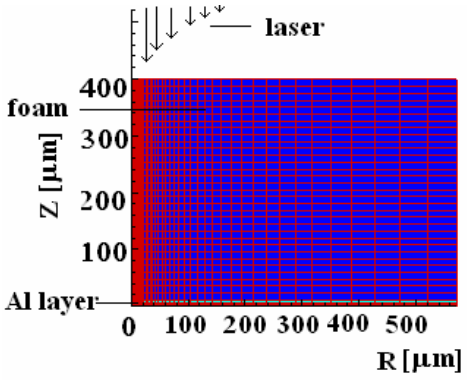


Fig.9b. Contours of the numerical grid.

Fig.10 illustrates the results of 2D numerical simulations (variant 15a_2D).

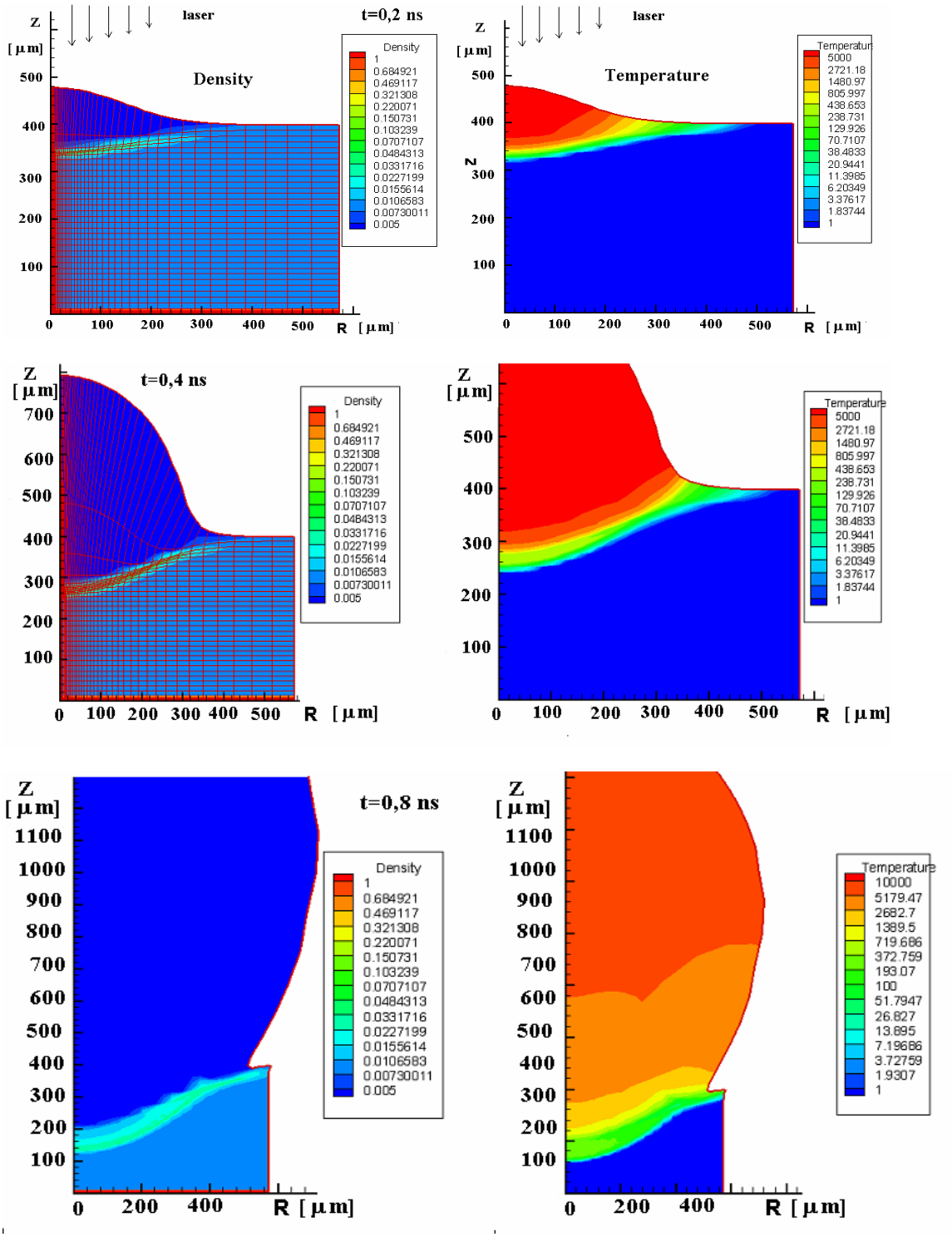


*Fig.10. The shapes of densities (left) and temperatures (right) fields at t=0.2, 0.4 and 0.8 ns. Initial density of matter is $\rho_0$=9 mg/cm$^3$.*

Figure 11 illustrates results of 2D calculations: the wave propagation along 0Z axis for different initial densities of low density matter:

a) $\rho_0$=4.5 mg/cm$^3$ (**var. 25a)** **b)** $\rho_0$=9 mg/cm$^3$ (v**ar. 15a)** **c)** $\rho_0$=9 mg/cm$^3$(**var.24a**).

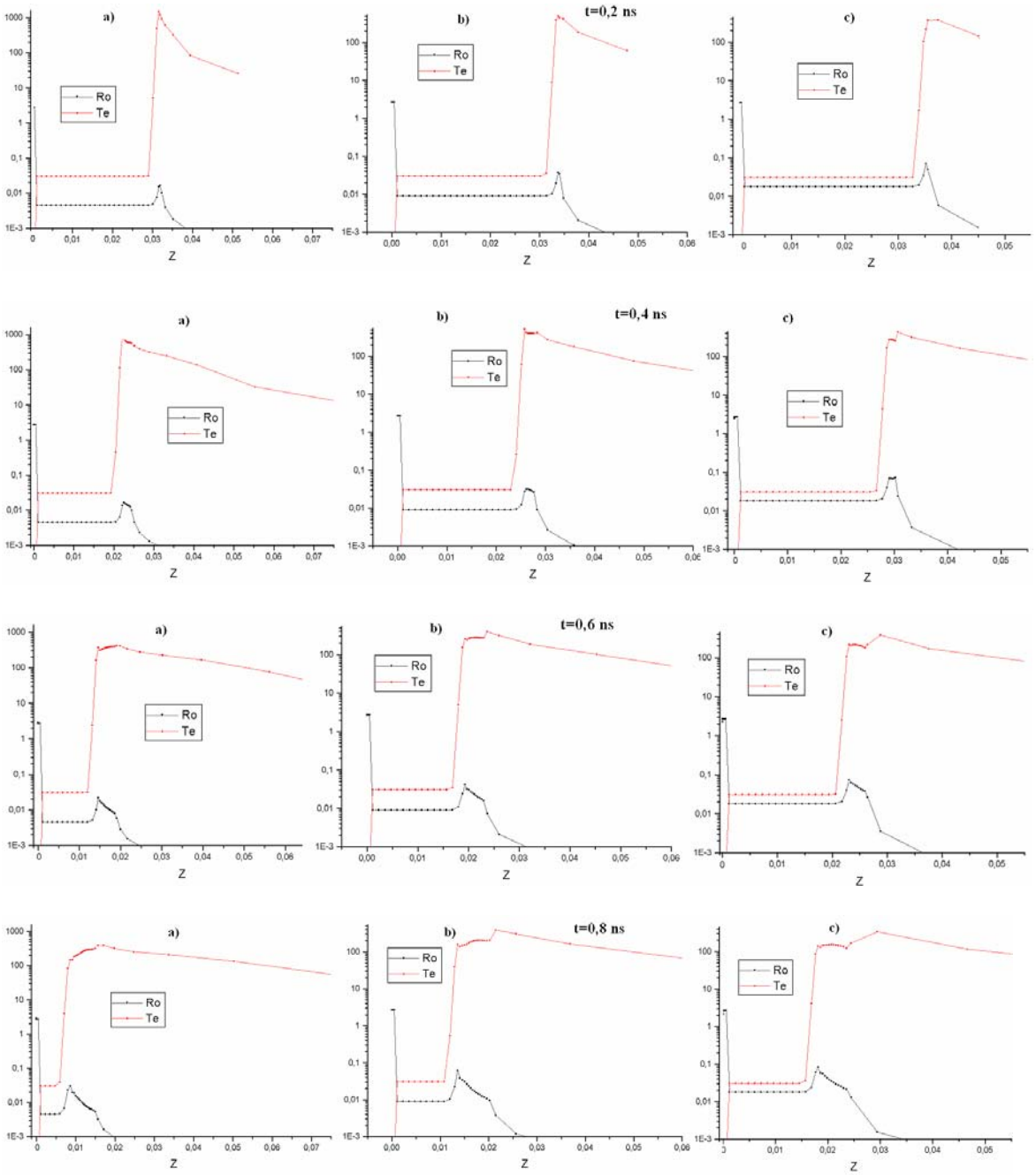


*Fig. 11. The distributions of density (black line) and temperature (red line) at t=0.2, 0.4, 0.6 and 0.8 ns.*

The average velocities of wave propagation in low-density matter are $\overline{V} = 516$ km/s ($\rho_0$=2.25 mg/cm$^3$), $\overline{V} = 410$ km/s ($\rho_0$=4.5 mg/cm$^3$), $\overline{V} = 337$ km/s ($\rho_0$=9 mg/cm$^3$) and $\overline{V} = 279$ km/s ($\rho_0$=18 mg/cm$^3$).

We have supposed the Equation of State (EOS) in porous matter is perfect gas with adiabatic index $\gamma$=5/3. In this case the temperature in plasma is much larger then 1 keV.

We have supposed that thermal capacity is higher in two times: $C_V = 3k_B$, where $k_B$- is Boltzmann constant. It suits the adiabatic index $\gamma$=4/3. In this set of simulations we have corrected the coefficient of laser absorption: $\chi_L = \dfrac{\rho(z,t)}{\rho_{cr} l_a}$, where $\rho_{cr}$ – critical density. It allows to use only a single "free parameter" – $l_a$.

We have calculated the variants: 26e ($\rho_0$=2.25 mg/cm$^3$), 25e ($\rho_0$=4.5 mg/cm$^3$), 15e ($\rho_0$=9 mg/cm$^3$) and 24e($\rho_0$=18 mg/cm$^3$) in "quasi-1D" approximations. The wave velocities have decreased and plasma temperatures have decreased too. Figure 12 illustrates comparison of wave propagation along the 0Z axis (variants: 15a ($\gamma_1$ = 5/3) and 15e ($\gamma_1$ = 4/3), and initial densities in both variants: $\rho_0$=9 mg/cm$^3$).

**·$\gamma_1$ = 5/3 (variant 15a_2D).** **·$\gamma_2$ = 4/3 (variant 15e_2D)**

**t = 0.2 ns**

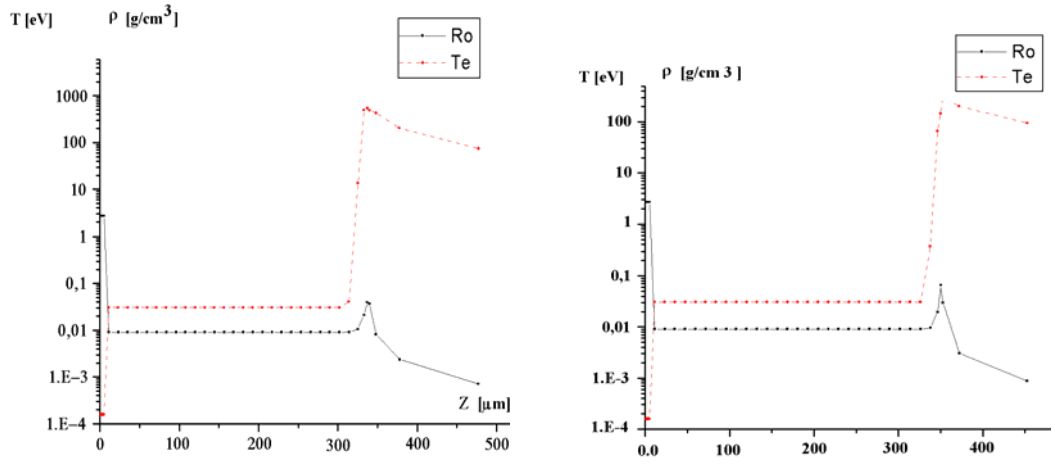

**t = 0,4 ns**

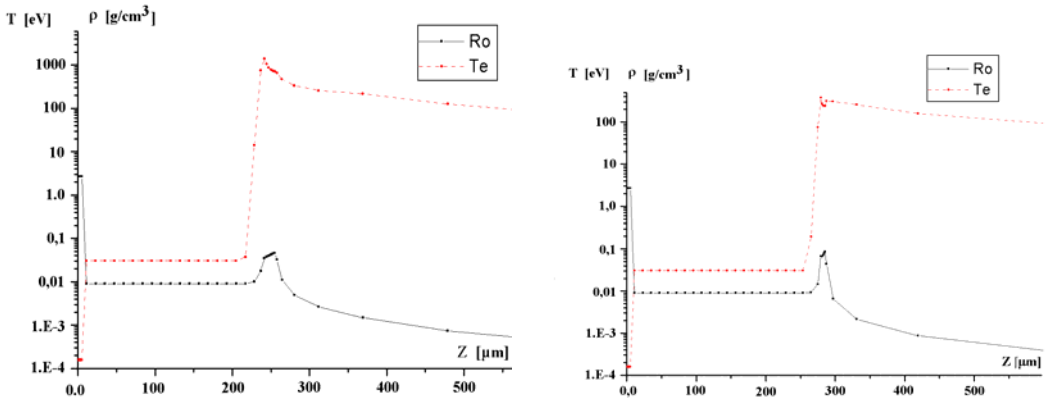


**t = 0,6 ns**

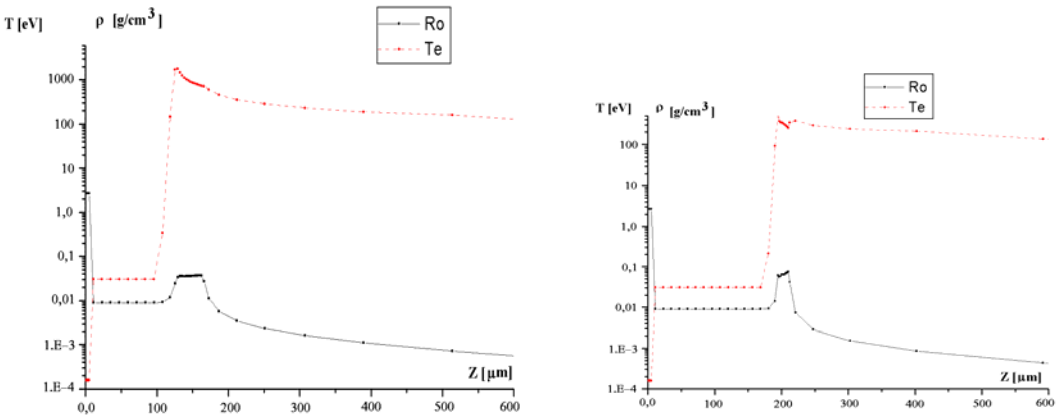


**t = 0,8 ns**

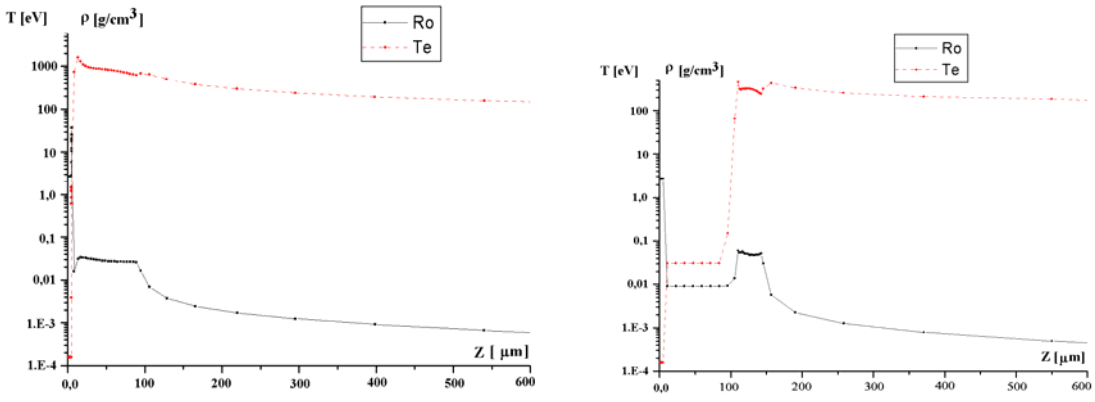


*Fig.12. The density (black line) and temperature (red line) distributions along 0Z axis in 1D geometry at the moments t=0.2, 0.4, 0.6 and 0.8 ns.*

The average velocities for the variant 15a $\overline{V} \approx 520$ км/s and for variant 15e: $\overline{V} \approx 360$ км/s ($\rho_0$=9 mg/cm$^3$). The temperature after wave front has decreased (in variant 15e). For a example, the temperature after wave front in plasma with γ=5/3 is Te≈ 1.3-1.5 keV and Te≈ 0.4-0.5 keV for γ=4/3.

We have made also 2D simulations with "Gaussian laser flux distribution: $q_2(r) = C / \exp(r / R_f)^2$, where C – normalized factor ( $\int_0^{R_0} q_2(r) r dr = 1$, $R_f = 150$ μm and $R_0 = 600$ μm.

With allowance for 2D effects the average velocity ($\overline{V}$) has been decreased approximately in (1,3-1,5) times.

The next figure illustrates the dependence of average velocities ($\overline{V}$) from initial densities ($\rho_0$).

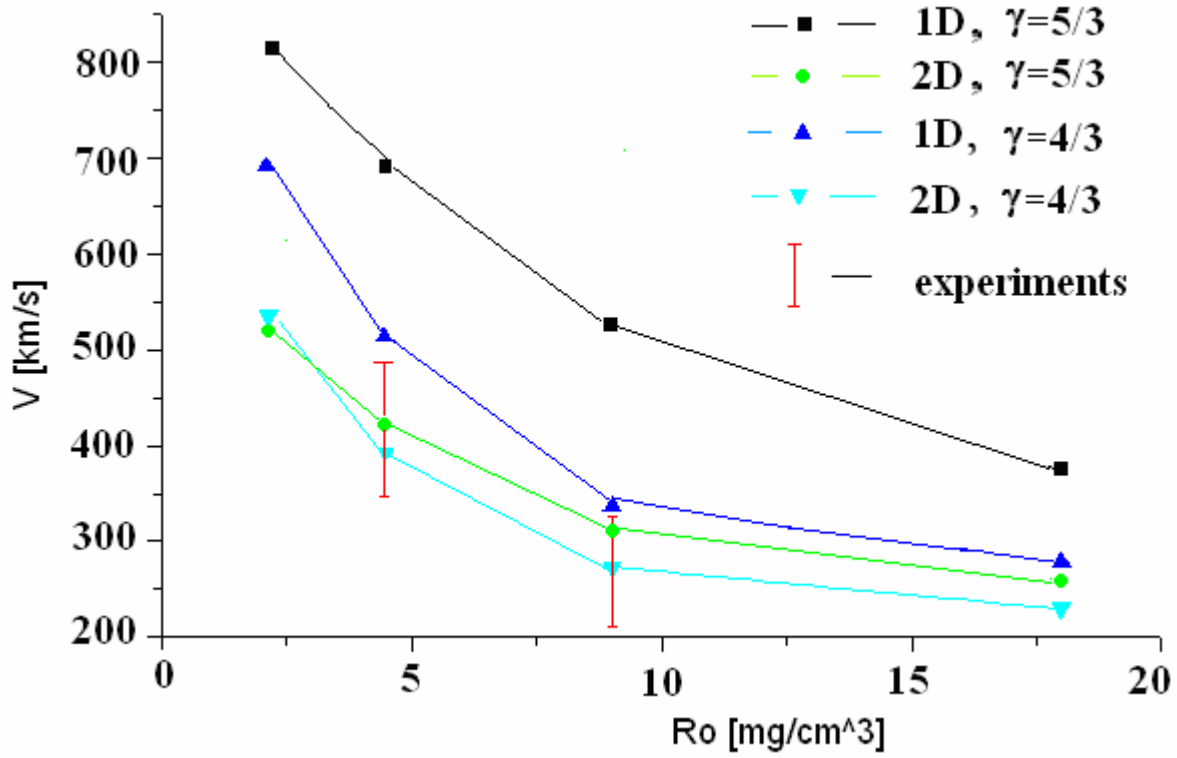


*Fig.13. Dependence of velocity of wave propagation as function of initial density. Vertical red lines are the experimental data.*

The red vertical lines are the results of experimental measurements (see [2]). It can see a good agreement between numerical and experimental results. If we suppose, that $\overline{V} \approx 272\left(\frac{9}{\rho_0}\right)^{\alpha}$, where density in [mg/cm3] and velocity in [km/s], then it can estimate $\alpha \approx (0.25 - 0.45)$ for our conditions.

A some interesting effect has been observed in the experiments with undercritical plasma at "PALS" installation. The part of laser energy has come through the low density matter and heated the Al foil in the beginning of laser pulse. We have supposed that in the period of 0<t<0,2 ns the low-density matter is transparent. As the results, about 3% of laser energy is heated Al layer (see Table 1).

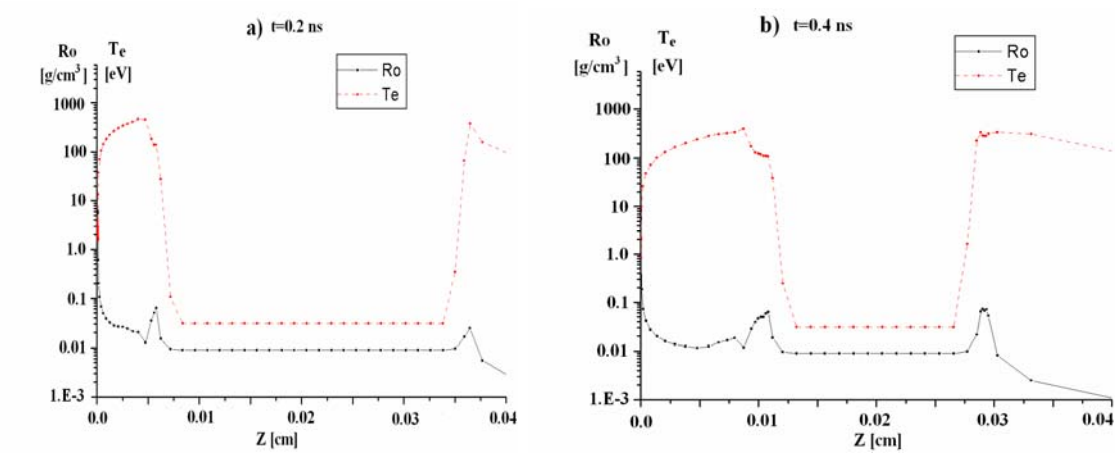


Fig. 14a,b. The density and temperature distribution along 0Z axis at the moment t=0.2 ns (a) and 0,4 ns (b).

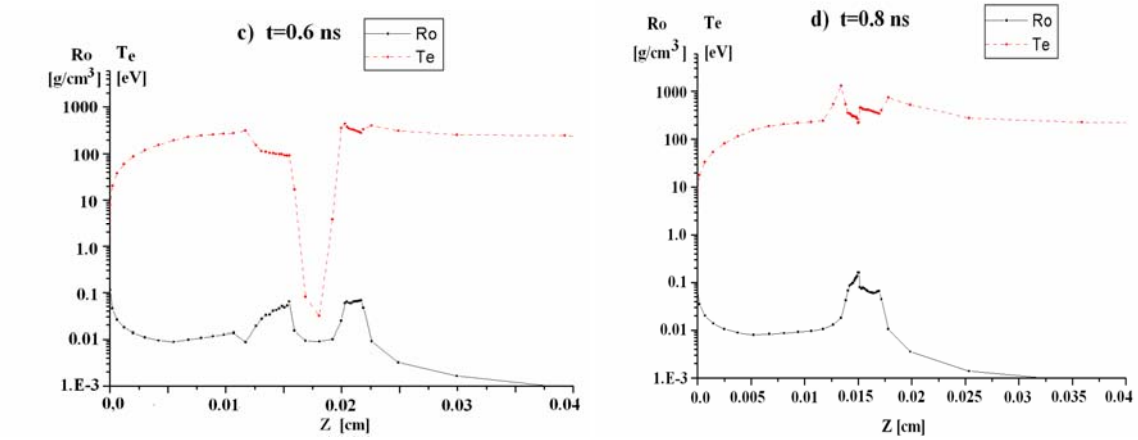


Fig. 14c,d. The density and temperature distribution along 0Z axis at the moment t=0.6 ns (c) and t=0.8 ns (d).

Fig.14-15 illustrates the results of 1D calculations (variant 15i_1D). Initial density of porous matter is $\rho_0$=9 mg/cm$^3$, $\gamma$=4/3. At the moment t≈ 0.7 ns, it can see the "flows collision": evaporated part of Al foil and "hydro-thermal wave", which has initiated by laser pulse. The energy of hydro-thermal wave higher, then the energy of evaporated layers of aluminium, so the wave moves to left. Fig.15 illustrates the evolution of hydro-thermal wave, when laser pulse has been finished. It shows the density and temperature distributions along 0Z axis at t=0.8, 1.4 and 2 ns. It is more convenient to show this Figure in mass cord, because the mass of Al layer is bigger then mass of porous matter, but the size is much less. The wave reaches the rear side of the target at t≈2 ns (see Fig.15c).

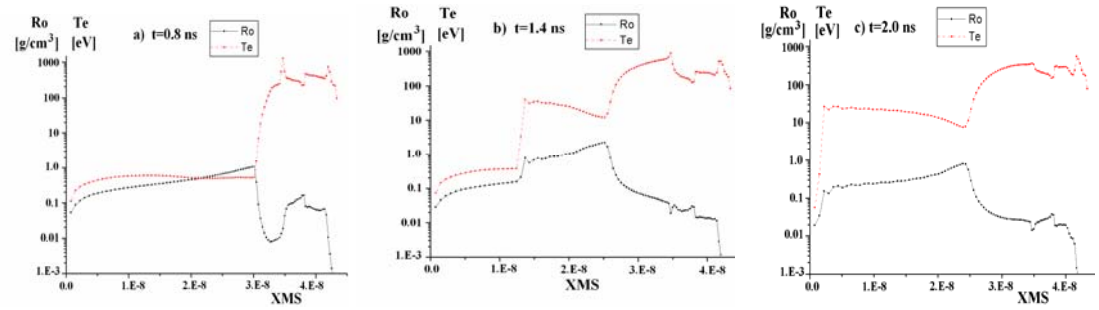


Fig.15. Dependence of density and temperature from mass cords. Hydro-wave front comes to left boundary to the moment t= 2 ns (!).

## Conclusions.

1. We have proposed a new model of formation and propagation of hydro-thermal wave in low density matter;
2. As the thickness of porous layer is equal or larger then diameter of focal spot it needs take into account two-dimensional effects in the model;
3. we have curried out 2D simulations by using Lagrange code "ATLANT" with allowance for new model of laser absorption and have got good agreements between the numerical calculations and the measurement of wave velocities in low-density matter;

4. an effect of Al base preheating and two flow collision has been modelled in our simulations. This effect can explain the delay of X-ray signal from rear boundary of target, which has observed in experiments.

## References.


1. Jungwirth K., Cejnarova A., Juha L. et al. The Prague Asterix Laser System. // Phys. Plasmas, 2001, v.8., pp.2495-3006
2. Akunetz A.A., Borisenko N.G., Klir D et al. Osobennosti prohozhdenija lazernogo izluchenija c dlinoj volni 0,438 mkm i intensivnostju (3-7)$10^{14}$ W/$cm^2$ cherez podkriticheskuju plazmu iz polimernih aerogeley. Preprint of Lebedev Physical Institite RAS, #8, Moscow, 2007 (in Russian).